

Polymer and Hybrid Electron Accepting Materials Based on a Semiconducting Perfluorophenylquinoline

Andreas A. Stefopoulos,^{†,§} Souzana N. Kourkouli,^{†,§}
Solon Economopoulos,[†] Fotini Ravani,[§]
Aikaterini Andreopoulou,[†] Kostas Papagelis,[‡]
Angeliki Siokou,[§] and Joannis K. Kallitsis^{*,†,§}

[†]Department of Chemistry, and [‡]Department of Materials Science, University of Patras, Patras GR26504, Greece,
[§]Foundation for Research and Technology Hellas, Institute of Chemical Engineering and High Temperature Processes (FORTH-ICEHT), Patras GR26504, Greece, and [‡]Theoretical and Physical Chemistry Institute, National Hellenic Research Foundation, Athens GR11635, Greece

Received April 30, 2010

Revised Manuscript Received May 3, 2010

Recent progress in organic polymer photovoltaics (OPVs) has been realized mainly through the development of low band gap semiconducting donors, morphology control of donor–acceptor nanophase separation, charge mobility increment, and device optimization.¹ In most of these efforts, PCBM ([6,6]-phenyl C61 butyric acid methyl ester) was used as the electron accepting material.^{2,3} On the contrary, the development of efficient polymer electron acceptors has not yet attracted the analogous attention. Working in this direction we have synthesized a new electron accepting polymeric perfluorophenylquinoline (P5FQ). In order to create materials of increased electron affinity, the hybrid SWCNTs-*graft*-P5FQ has also been developed. The modification of polyquinolines⁴ toward lower LUMO values will increase their electron accepting properties, and moreover their attachment onto SWCNTs⁵ should highly benefit the system's electron transport characteristics.

A perfluorophenylvinylphenylquinoline monomer was synthesized via the Friedländer procedure followed by a typical Suzuki reaction leading to the final vinylic monomer 5FQ (Scheme S1, Figure S2). Homopolymers P5FQ of this perfluorophenylvinylphenylquinoline were prepared through free radical polymerization (FRP), presenting excellent solubilities in most common organic solvents (Scheme 1, Table S1, Figure S3). The same monomer 5FQ was used in atom transfer radical polymerization (ATRP) employing an initiator based on properly modified SWCNTs (Scheme S2,⁶ Scheme 1).

In this case, SWCNTs were hydroxyl functionalized via the diazonium chemistry, reported from Tour et al.,⁷ using 4-aminophenol and isopentyl nitrite (Scheme S2). Based on thermogravimetric analysis, efficient hydroxyl functionalization of the single wall carbon nanotubes (SWCNT-OH) was obtained (Figure S4) with a 21% weight of the functionalized nanotubes corresponding to the attached phenol groups; thus, one functional group was attached onto every 32 carbon atoms. Raman spectroscopy was used to clarify the covalent attachment of the phenol groups (Figure S5). The ratio I_D/I_G^+ of the pristine SWCNTs and SWCNT-OH sample (Table S2) shows that the intensity of the D-band increases considerably upon functionalization (Figure S5a). In the second step, the SWCNT-OH was esterified with 2-chloropropionyl chloride in order to create

ATRP initiator sites on the nanotubes surface (SWCNT-Init) (Scheme S2). TG analysis showed an additional weight loss of 10% corresponding to the 2-chloropropionyl group attached with an ester bond on the SWCNT-OH phenols (Figure S4). Employing ATRP conditions,⁸ we successfully polymerized monomer 5FQ onto the SWCNT surface affording SWCNT-*g*-P5FQ polymer–nanotube hybrid materials (Scheme 1). The degree of the polymerization was estimated from TG analysis of the polymer functionalized carbon nanotubes (Figure S4) showing an 18% additional weight loss compared to the SWCNT-Init. For better qualification of the polymerization the Raman spectrum collected for the SWCNT-*g*-P5FQ sample is included in Figure S5. The hydroxyl functionalized and polymer modified tubes exhibit almost similar intensity ratio I_D/I_G^+ (Table S1). This indicates that the polymerization of the 5FQ monomer takes place solely from the surface-derived initiators on SWCNTs. In other words, it seems that the number of grafted sites on the nanotubes remains constant during polymerization, justifying the “grafting from” strategy employed in the present study. The UV–vis characterization of the homopolymer P5FQ (Figure S7) revealed upon protonation with formic acid a red shift and quenching of the PL intensity due to excimer formation of the quinoline units. In addition to our previous reported work,⁶ the immobilization of the quinoline oligomers onto the carbon nanotube surface makes them unable to create excimers even though they are protonated, and thus there is no quenching of their photoluminescence. The photoluminescence examination

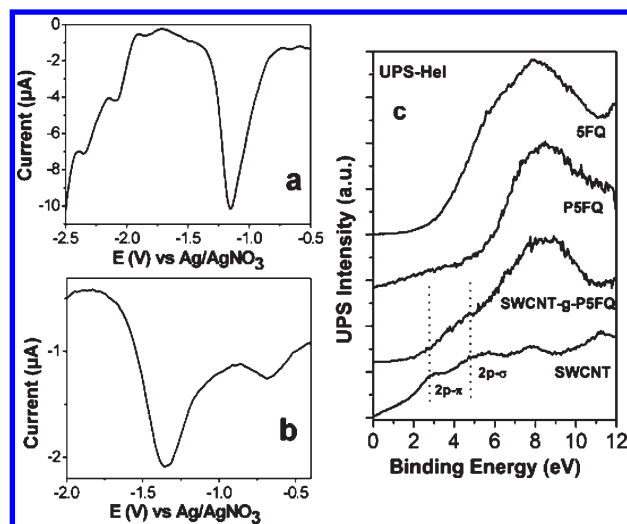
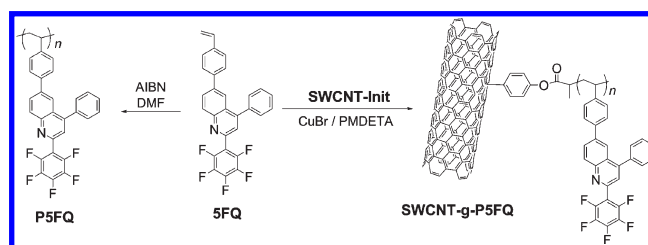


Figure 1. Differential pulse voltammograms (reduction runs) obtained in TBAPF₆ 0.1 M in DMF of (a) quinoline polymer P5FQ and (b) hybrid material SWCNT-*g*-P5FQ. (c) UPS spectra.

Scheme 1. Synthetic Routes to Homopolymers P5FQ and Hybrid SWCNT-*g*-P5FQ Materials



*Corresponding author: e-mail j.kallitsis@upatras.gr, Tel +30-2610962952, Fax +30-2610997122.

Table 1. Electronic Properties of the Monomer, Polymer, and Hybrid Perfluorophenylquinolines

	$E_{1,\text{red}}$ (V)	$E_{2,\text{red}}$ (V)	$E_{3,\text{red}}$ (V)	E_g (opt-sol) (eV)	E_g (opt-film) (eV)	HOMO (UPS) (± 0.1 eV)	LUMO (CV) (eV)
5FQ	−1.52	−2.08	−2.32	3.3	3.2	6.2	3.27
P5FQ	−1.15	−2.08	−2.33	3.2	3.1	6	3.65
SWCNT- <i>g</i> -P5FQ	−0.68	−1.34				5.3	

of SWCNT-*g*-P5FQ in DMF and in formic acid (Figure S8) produced spectra, with the same intensity and with no red shift for the protonated sample.

Electrochemistry conducted on the newly synthesized materials showed three redox processes for the monomer 5FQ (Figure S9) at $E_{1/2} = -1.52$ V, $E_{1/2} = -2.08$ V, and $E_{1/2} = -2.32$ V vs Ag/AgNO₃. This data reveals an electron affinity for the monomer 5FQ around 3.27 eV, in good accordance with the data obtained by the UPS experiments. It is also worth noting that it is one of the lowest lying LUMO reported for a nonconjugated quinoline molecule. In Figure 1a,b the DPV reduction runs of polymer P5FQ and hybrid material SWCNT-*g*-P5FQ are presented. In Figure 1a the polymer P5FQ exhibits a main reduction process at −1.15 V anodically shifted by ~350 mV compared to monomer 5FQ yielding a LUMO of 3.65 eV.

This LUMO value is considerably lower than the one at 2.5 eV obtained for the unsubstituted polyquinolines reported previously.⁹ Two weaker peaks are also present at −2.08 and −2.33 V. Both of these peaks present a negligible anodic shift compared to the monomers DPV in Figure S9. In Figure 1b material SWCNT-*g*-P5FQ is examined where two main reduction peaks are easily observable: one at −1.34 V attributed to the P5FQ polymer and a broad weak signal, characteristic of SWCNTs, at −0.68 V. The peak at −1.34 V is cathodically shifted compared to the pristine P5FQ polymer by almost 200 mV, suggesting that electronic interactions are taking place between the quinoline and the SWCNT. Figure 1c shows the UPS-derived valence band spectra from the four samples, i.e., the pristine SWCNTs, the polymer modified SWCNT-*g*-P5FQ, the homopolymer P5FQ, and the monomer 5FQ. The prominent features at the valence band spectrum of the SWCNT originate from the 3-fold coordination of the C atoms. These are the 2p- π band near 3 eV (sp^2 hybridization), the 2p- σ states near 5.5 and 8.0 eV, and the mixed 2s-2p hybridized states at 12 eV.¹⁰ In the case of the homopolymer P5FQ and the monomer 5FQ the density of states near the Fermi level is dramatically reduced while the main feature in their spectra is the wide band at 8.3 eV (carbon 2p- σ states). Finally, at the hybrid material SWCNT-*g*-P5FQ, the peak originating from the carbon nanotubes 2p- σ (originally at 5.5 eV) has a 0.5 eV red shift while the intensity of the 2 π -p band at 3 eV has been suppressed due to the interaction between the nanotubes and the homopolymer. Summarized data of DPV and UPS experiments are given in Table 1.

The obtained LUMO value for the P5FQ polymer is well comparable to or even better than the best so far reported polymeric or small molecule electron acceptors.^{11,12} The presence of the SWCNTs on the electron acceptor phase could significantly contribute to the efficient transport of the separated electrons to the respective electrode. Another key advantage of this approach is that it is based on an electron accepting vinylic monomer which can be incorporated in more complex polymeric architectures like rod-coil block copolymers or polymeric brushes having characteristics of both electron acceptor and donor. It also can be combined with well-known electron acceptor

nanomaterials like [60]fullerene derivatives in a hybrid-polymeric architecture. Work in this direction is currently in progress.

Acknowledgment. Partial support from the projects CNTCOMP of the Marie Curie Actions (MTKD-CT-2005-029876) by the European Union and the Heraclitus II Program for Basic Research and the Hellenic Ministry of Education is greatly acknowledged.

Supporting Information Available: Experimental procedures, ¹H and ¹³C NMR, TGA, Raman, UV-vis-NIR, UV-vis, PL, and DPV characterization of all prepared materials. This material is available free of charge via the Internet at <http://pubs.acs.org>.

References and Notes

- (1) (a) Kim, J. Y.; Lee, K.; Coates, N. E.; Moses, D.; Nguyen, T.-Q.; Dante, M.; Heeger, A. J. *Science* **2007**, *317*, 222–225. (b) Yu, G.; Gao, J.; Hummelen, J. C.; Wudl, F.; Heeger, A. J. *Science* **1995**, *270*, 1789–1791. (c) Park, S. H.; Roy, A.; Beaupré, S.; Cho, S.; Coates, N.; Moon, J. S.; Moses, D.; Leclerc, M.; Lee, K.; Heeger, A. J. *Nat. Photonics* **2009**, *5*, 296–302.
- (2) (a) Chen, J.; Cao, Y. *Acc. Chem. Res.* **2009**, *42*, 1709–1718. (b) Peet, J.; Heeger, A. J.; Bazan, G. C. *Acc. Chem. Res.* **2009**, *42*, 1700–1708.
- (3) (a) Ago, H.; Petritsch, K.; Shaffer, M. S. P.; Windle, A. H.; Friend, R. H. *Adv. Mater.* **1999**, *11*, 1281–1285. (b) Li, C.; Chen, Y.; Wang, Y.; Iqbal, Z.; Chhowalla, M.; Mitra, S. J. *Mater. Chem.* **2007**, *17*, 2406–2411. (c) Cioffi, C.; Campidelli, S.; Sooambar, C.; Marcaccio, M.; Marcolongo, G.; Meneghetti, M.; Paolucci, D.; Paolucci, F.; Ehli, C.; Rahman, G. M. A.; Sgobba, V.; Guldi, D. M.; Prato, M. *J. Am. Chem. Soc.* **2007**, *129*, 3938–3945.
- (4) (a) Jenekhe, S.; Chen, X. *Science* **1998**, *279*, 1903–1907. (b) Jenekhe, S.; Chen, X. *Science* **1999**, *283*, 372–375.
- (5) (a) Kanungo, M.; Lu, H.; Malliaras, G. G.; Blanchet, G. B. *Science* **2009**, *323*, 234–237. (b) Tasis, D.; Tagmatarchis, N.; Bianco, A.; Prato, M. *Chem. Rev.* **2006**, *106*, 1105–1136. (c) Campidelli, S.; Ballesteros, B.; Filoramo, A.; Diaz Diaz, D.; De la Torre, G.; Torres, T.; Rahman, G. M. A.; Ehli, C.; Kiessling, D.; Werner, F.; Sgobba, V.; Guldi, D. M.; Cioffi, C.; Prato, M.; Bourgoign, J.-P. *J. Am. Chem. Soc.* **2008**, *130*, 11503–11509.
- (6) (a) Chochos, C. L.; Stefopoulos, A. A.; Campidelli, S.; Prato, M.; Gregoriou, V. G.; Kallitsis, J. K. *Macromolecules* **2008**, *41*, 1825–1830. (b) Liu, Y.; Yao, Z.; Adronov, A. *Macromolecules* **2005**, *38*, 1172–1179.
- (7) (a) Hudson, J.; Casavant, M.; Tour, J. J. *J. Am. Chem. Soc.* **2004**, *126*, 11158–11159. (b) Usrey, M. L.; Lippmann, E. S.; Strano, M. S. *J. Am. Chem. Soc.* **2005**, *127*, 16129–16135.
- (8) (a) Yao, Z.; Braid, N.; Botton, G. A.; Adronov, A. *J. Am. Chem. Soc.* **2003**, *125*, 16015–16024. (b) Kong, H.; Gao, C.; Yan, D. Y. *J. Am. Chem. Soc.* **2004**, *126*, 412–413.
- (9) Economopoulos, S. P.; Andreopoulou, A. K.; Gregoriou, V. G.; Kallitsis, J. K. *Chem. Mater.* **2005**, *17*, 1063–1071.
- (10) Chen, P.; Wu, X.; Lin, J.; Li, H.; Tan, K. L. *Carbon* **2000**, *38*, 139–143.
- (11) (a) Kietzke, T.; Horhold, H. H.; Neher, D. *Chem. Mater.* **2005**, *17*, 6532–6537. (b) Chochos, C. L.; Economopoulos, S. P.; Deimede, V.; Gregoriou, V. G.; Lloyd, M. T.; Malliaras, G. G.; Kallitsis, J. K. *J. Phys. Chem. B* **2007**, *111*, 10732–10740. (c) Alam, M. M.; Jenekhe, S. A. *Chem. Mater.* **2004**, *16*, 4647–4656.
- (12) Brunetti, F. G.; Gong, X.; Tong, M.; Heeger, A. J.; Wudl, F. *Angew. Chem., Int. Ed.* **2010**, *49*, 532–536.